A Theory of Steady Wind-Driven Currents in Shallow Water with Variable Eddy Viscosity

JOHN H. THOMAS

Dept. of Mechanical and Aerospace Sciences, University of Rochester, Rochester, N. Y. 14627

(Manuscript received 2 May 1974, in revised form 26 September 1974)

ABSTRACT

A theory is given for steady wind-driven currents in shallow water (friction depth comparable to total depth) in which the vertical eddy viscosity varies linearly with depth, from zero at the bottom to a maximum at the surface. The theory is presented in a form suitable for numerical computations of currents in real, enclosed basins. The local surface value of the vertical eddy viscosity depends on the surface wind stress, the bottom roughness, and the flow itself; this leads to a quasi-linear equation for the determination of the surface slope or the vertically-integrated mass flux. Results are given for the simple case of a pure drift current in water of uniform depth, and these results are compared with those for a constant vertical eddy viscosity.

1. Introduction

Welander (1957) developed a theory of wind-driven currents and surface displacements in a shallow body of water—shallow in the sense that the friction depth is comparable to the total depth. This theory is basically an extension of Ekman's (1905) analysis to the case of finite depth. Recently, Welander's theory has been successfully applied in numerical modeling of wind-driven currents in the North American Great Lakes, first by Gedney and Lick (1972) for Lake Erie, and then by Bonham-Carter and Thomas (1973) for Lake Ontario. The shallow-water theory involves several approximations, including the neglect of both internal friction and nonlinear acceleration terms. However, as Welander himself points out, the most unrealistic assumption is that of constant vertical eddy viscosity. The present paper deals with a formulation of shallow-water theory under a more realistic assumption about the behavior of the vertical eddy viscosity.

Both theory and experiment suggest that the vertical eddy viscosity ν should depend on the flow itself, and that in general it should vary from a maximum at or near the free surface to zero at the bottom. As a simple model of this expected behavior, we assume here that ν varies linearly from a maximum ν_0 at the surface to zero at the bottom. This form of variation is defensible on both theoretical and experimental grounds and leads, as we shall see, to a formulation of shallow-water theory which is suitable for numerical modeling of real basins.

This linear variation of ν with depth is intended only to model a homogeneous, unstratified body of water. In the case of strong thermocline conditions typical of many large lakes in midsummer, a two-layer shallow-water model can be used (Gedney *et al.*, 1972), and in this case the linear variation of ν with depth might be appropriate for one or both layers.

Fjelstad (1929), using observations of currents on the North Siberian Shelf made by Sverdrup, found that the variation of eddy viscosity with depth was described closely by a power law with $\nu \propto z^{\frac{1}{2}}$. This is reasonably close to the form $\nu \propto z$ suggested here. However, Fjelstad's analysis assumes that the observed current was a pure wind-drift current, with no contribution due to horizontal pressure gradients (surface slopes). It is difficult to determine to what extent horizontal pressure gradients may have contributed to the flow. Ideally, assumptions about the variation of eddy viscosity with depth should be tested under controlled laboratory conditions.

Ellison (1956) analyzed the atmospheric boundary layer between the ground and a uniform geostrophic wind, under the assumption that the eddy viscosity varies with height. Recent laboratory studies of the turbulent Ekman layer by Caldwell *et al.* (1972) have shown Ellison's theory to be in good agreement with experiment. It was Ellison's work which suggested the present approach to shallow-water theory.

A continuous increase in eddy viscosity from bottom to top is to be expected for two reasons: (i) vertical eddying motions are inhibited near the rigid bottom, and (ii) the driving source of the turbulence, the surface wind stress, acts at the top. A linear increase in ν from zero at the bottom is equivalent to a mixing length theory of the bottom boundary layer, in which the mixing length is proportional to the distance from the bottom. This leads to a logarithmic behavior of the velocity near the bottom, and allows for the specifica-

tion of a "roughness length" to characterize the roughness of the bottom. Near the surface the behavior of ν presents a complicated problem, with both eddying motions and gravity waves contributing to the Reynolds shear stress. The linear variation of ν seems a reasonable approximation here.

In the next section we formulate the theory of steady wind-driven currents with our assumed behavior of ν, in a form suitable for numerical modeling of real, enclosed bodies of water with variable bottom topography. One important result is that the maximum eddy viscosity ν_0 depends on the surface wind stress, the bottom topography, and the flow itself, and cannot be specified independently as it can in the case of constant ν. Although the analysis of flow problems is greatly complicated, this dependence of ν on the flow is certainly a more realistic situation.

In Section 3 we consider the simple case of a pure drift current (no surface slope) in water of uniform depth. The resulting velocity distribution is compared with the velocity distribution for the case of constant ν, i.e., the classical Ekman spiral for finite depth.

2. Analysis

We assume that the lateral dimensions of the body of water are large compared with the depth, but are small enough that we can ignore the effects of the earth's curvature, including the variation of the Coriolis parameter with latitude. We thus make the "tangent plane" approximation, and choose a Cartesian coordinate system $\hat{x}$, $\hat{y}$, $\hat{z}$ (the carets denote dimensional quantities) fixed relative to the rotating earth, with the $\hat{z}$ axis vertically upward and the origin at the undisturbed water surface (see Fig. 1).

We also assume that the water is homogeneous, that the pressure distribution is hydrostatic, and that the lateral friction and nonlinear acceleration terms are negligible [for a scale analysis to justify these approximations for large lakes, see Gedney and Lick (1972) or Bonham-Carter and Thomas (1973)]. The surface atmospheric pressure is assumed to be uniform. The vertical eddy viscosity is allowed to vary with depth. The basic equations, then, are the continuity equation

$$\frac{\partial \hat{u}}{\partial \hat{x}}+\frac{\partial \hat{v}}{\partial \hat{y}}+\frac{\partial \hat{w}}{\partial \hat{z}}=0, \tag{1}$$

and the horizontal momentum equations

$$-f\hat{v}=-g\frac{\partial \hat{\zeta}}{\partial \hat{x}}+\frac{\partial}{\partial \hat{z}}\left(\nu\frac{\partial \hat{u}}{\partial \hat{z}}\right), \tag{2}$$

$$f\hat{u}=-g\frac{\partial \hat{\zeta}}{\partial \hat{y}}+\frac{\partial}{\partial \hat{z}}\left(\nu\frac{\partial \hat{v}}{\partial \hat{z}}\right). \tag{3}$$

Here $\hat{\mathbf{u}}=(\hat{u},\hat{v},\hat{w})$ is the dimensional velocity, g the acceleration of gravity, f the Coriolis parameter,

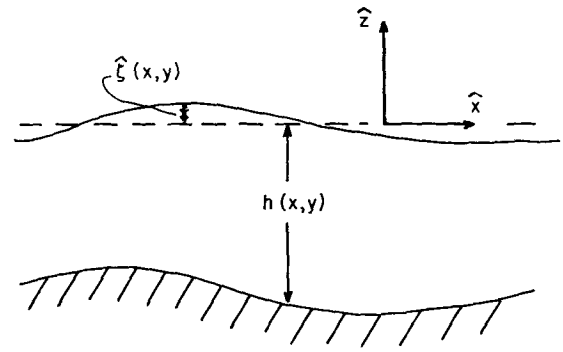

FIG. 1. Basic coordinate system.

$\nu=\nu(\hat{z})$ the vertical eddy viscosity, and $\hat{\zeta}=\hat{\zeta}(\hat{x},\hat{y})$ the displacement of the free surface. Eqs. (2) and (3) can be conveniently combined into the single complex equation

$$\frac{\partial}{\partial \hat{z}}\left(\nu\frac{\partial \hat{\phi}}{\partial \hat{z}}\right)-if\hat{\phi}=g\frac{\partial \hat{\zeta}}{\partial \hat{n}}, \tag{4}$$

where $\hat{\phi}=\hat{u}+i\hat{v}$ and $\partial/\partial\hat{n}=\partial/\partial\hat{x}+i\partial/\partial\hat{y}$.

Now, we take $\nu(\hat{z})$ in the form

$$\nu=\nu_0\left(1+\frac{\hat{z}}{h}\right)=ku_*(h+\hat{z}); \tag{5}$$

that is, ν varies linearly from zero at the bottom ($\hat{z}=-h$) to a maximum ν_0 at the surface ($\hat{z}=0$). Here, $u_*=\nu_0/(kh)$ is the friction velocity and k an empirical constant ($k\approx 0.4$), both being familiar in turbulent boundary layer theory. In a basin of variable depth, $h=h(\hat{x},\hat{y})$, ν will vary horizontally as well as vertically. With the form (5) for $\nu(\hat{z})$, Eq. (4) becomes

$$\nu_0\frac{\partial}{\partial \hat{z}}\left[\left(1+\frac{\hat{z}}{h}\right)\frac{\partial \hat{\phi}}{\partial \hat{z}}\right]-if\hat{\phi}=g\frac{\partial \hat{\zeta}}{\partial \hat{n}}. \tag{6}$$

We now put Eq. (6) in nondimensional form. Let L be the horizontal length scale of the basin, and define

$$\left.\begin{aligned} x=\hat{x}/L,\quad y=\hat{y}/L,\quad \frac{\partial}{\partial n}=\frac{\partial}{\partial x}+i\frac{\partial}{\partial y}=L\frac{\partial}{\partial \hat{n}} \\ z=\hat{z}/h,\quad \zeta=\frac{g}{fu_*L}\hat{\zeta} \\ u=\hat{u}/u_*,\quad v=\hat{v}/u_*,\quad \phi=\hat{\phi}/u_* \end{aligned}\right\}.$$

Although u_* varies with horizontal position in a basin with variable depth, we use some fixed value in the above scaling. In terms of nondimensional quantities, Eq. (6) becomes

$$\frac{\partial}{\partial z}\left[(1+z)\frac{\partial \phi}{\partial z}\right]-i\alpha\phi=\alpha\frac{\partial \zeta}{\partial n}, \tag{7}$$

where the parameter $\alpha = fh^2/\nu_0$ is a reciprocal Ekman number. The surface boundary condition is, in dimensional form,

$$\rho\nu_0 \frac{\partial\hat{\phi}}{\partial\hat{z}}\bigg|_{\hat{z}=0} = \hat{\tau} = \hat{\tau}_x + i\hat{\tau}_y,$$

where ρ is the density and $\hat{\tau}$ the surface wind stress. Note that as usual this condition is applied at $\hat{z}=0$ rather than at the true free surface, $\hat{z}=\hat{\zeta}$; this leads to considerable simplification, and is consistent with other approximations we have made. In terms of dimensionless quantities, the surface condition is

$$\frac{\partial\phi}{\partial z}\bigg|_{z=0} = \alpha\tau, \tag{8}$$

where τ is the nondimensional surface wind stress defined as $\tau = \hat{\tau}/(\rho f h u_*)$.

We seek the solution of (7) satisfying (8), and having the proper logarithmic behavior near the bottom. With the change of variables $\eta = [4\alpha(1+z)]^{\frac{1}{2}}$, (7) becomes

$$\frac{\partial^2\phi}{\partial\eta^2} + \frac{1}{\eta}\frac{\partial\phi}{\partial\eta} - i\phi = \frac{\partial\zeta}{\partial n}, \tag{9}$$

and condition (8) becomes

$$\frac{\partial\phi}{\partial\eta}\bigg|_{\eta=\sqrt{4\alpha}} = \sqrt{\alpha}\tau. \tag{10}$$

The general solution of (9) is

$$\phi(\eta) = AI_0(i^{\frac{1}{2}}\eta) + BK_0(i^{\frac{1}{2}}\eta) + i\frac{\partial\zeta}{\partial n}, \tag{11}$$

where I_0 and K_0 are modified Bessel functions of first and second kind.

Near the bottom, we want the solution to have the turbulent boundary layer form

$$|\hat{\phi}| \sim \frac{u_*}{k}\ln\left(\frac{h+\hat{z}}{z_0}\right),$$

where z_0 is the roughness length. In nondimensional form, this becomes

$$|\phi| \sim \frac{1}{k}\ln\left(\frac{1+z}{\epsilon}\right) = \frac{1}{k}\ln\left(\frac{\eta^2}{4\alpha\epsilon}\right), \tag{12}$$

where $\epsilon = z_0/h$. Using the limiting form of the modified Bessel functions for small argument, we have from (11) for $\eta \sim 0$,

$$\phi(\eta) \sim A - B\left[\ln\left(\frac{\eta}{2}e^{i\pi/4}\right) + \gamma\right] + i\frac{\partial\zeta}{\partial n}, \tag{13}$$

where $\gamma = 0.57721$ is Euler's constant. Comparing (12) and (13), we see that we obtain the proper behavior at the bottom with

$$B = -\frac{2}{k}e^{i\theta_0}, \quad A = B\left(\frac{1}{2}\ln(\alpha\epsilon) + i\frac{\pi}{4} + \gamma\right) - i\frac{\partial\zeta}{\partial n}. \tag{14}$$

Here, θ_0 is the direction of the flow at the bottom, measured from the x axis. With the values of A and B in (14), the general solution (11) becomes

$$\phi(\eta) = -\frac{2}{k}e^{i\theta_0}\left\{\left[\frac{1}{2}\ln(\alpha\epsilon) + i\frac{\pi}{4} + \gamma\right] \times I_0(i^{\frac{1}{2}}\eta) + K_0(i^{\frac{1}{2}}\eta)\right\} + i\frac{\partial\zeta}{\partial n}[1 - I_0(i^{\frac{1}{2}}\eta)]. \tag{15}$$

The surface boundary condition (10) then becomes

$$-\frac{2}{k}i^{\frac{1}{2}}e^{i\theta_0}U(\alpha,\epsilon) + iV(\alpha)\frac{\partial\zeta}{\partial n} = \sqrt{\alpha}\tau, \tag{16}$$

where

$$\left.\begin{aligned} U(\alpha,\epsilon) &= \left\{\left[\frac{1}{2}\ln(\alpha\epsilon) + i\frac{\pi}{4} + \gamma\right]I_1(\sqrt{4i\alpha}) - K_1(\sqrt{4i\alpha})\right\} \\ V(\alpha) &= -i^{\frac{1}{2}}I_1(\sqrt{4i\alpha}) \end{aligned}\right\}. \tag{17}$$

Assuming the surface slope $\partial\zeta/\partial n$ at a fixed x, y point is known, (15) and (16) together determine the vertical distribution of horizontal velocity at that point. The procedure is as follows: the surface wind stress τ and the bottom roughness ϵ are specified, and then (16) provides a single complex equation for the determination of the two real quantities α and θ_0. Using the determined values of α and θ_0 in (15) gives the velocity distribution. Although (16) can be solved explicitly for θ_0, it is transcendental in α; thus, we cannot write a single explicit expression for the velocity distribution. Eq. (16) may be solved numerically by standard methods.

An important point here is that the value of α, and hence the value of ν_0 and u_*, is not specified independently; it is determined at each point as a function of the wind stress, surface slope and bottom roughness. This is quite different from the case of constant eddy viscosity, where the value of ν can be specified quite independently of the wind stress (although it shouldn't be). The present situation is more realistic—one expects the eddy viscosity to depend in some manner on the wind stress and flow. As a result of this dependence, ν_0 will vary with horizontal position x, y as well as depth z, even in a closed basin of constant depth.

TABLE 1. Values of α, h/D, τ, and the angles θ_0, θ_1 and θ (cf. Fig. 2) for $\epsilon = 0.01$.*

$\sqrt{4\alpha}$	α	h/D	τ	θ_0	θ_1	θ
0.4	0.04	0.064	1.01	− 8.22	− 6.92	− 1.30
0.8	0.16	0.127	1.13	− 30.64	−25.46	− 5.18
1.2	0.36	0.191	1.55	− 56.26	−44.63	− 11.63
1.6	0.64	0.255	2.35	− 75.97	−55.47	− 20.50
2.0	1.00	0.318	3.50	− 90.78	−59.26	− 31.52
2.4	1.44	0.382	5.01	−103.41	−59.20	− 44.21
2.8	1.96	0.446	6.94	−115.37	−57.42	− 57.95
3.2	2.56	0.509	9.38	−127.35	−55.21	− 72.14
3.6	3.24	0.573	12.50	−139.59	−53.20	− 86.39
4.0	4.00	0.637	16.53	−152.14	−51.67	−100.47
4.4	4.84	0.700	21.76	−164.93	−50.59	−114.34
4.8	5.76	0.764	28.63	−177.88	−49.87	−128.01
5.2	6.76	0.828	37.67	−190.90	−49.38	−141.52
5.6	7.84	0.891	49.61	−203.96	−49.03	−154.93
6.0	9.00	0.955	65.42	−217.00	−48.75	−168.25
6.8	11.56	1.08	114.28	−243.04	−48.30	−194.74
7.6	14.44	1.21	201.00	−269.04	−47.94	−221.10
8.4	17.64	1.34	356.38	−295.08	−47.63	−247.45
9.2	21.16	1.46	637.17	−321.26	−47.38	−273.88
10.0	25.00	1.59	1148.54	−347.67	−47.17	−300.50

* Angles in degrees.

We now turn to the problem of determining the surface slopes $\partial\zeta/\partial n$ in a closed basin. We introduce the nondimensional vertically-integrated volume flux $M = M_x + iM_y$, defined by

$$M = \int_{-1}^{0} \phi dz.$$

Using the basic equation (7) in this definition of M, we obtain

$$M = -\frac{i}{\alpha}\left(z\frac{\partial\phi}{\partial z}\right)\Big|_{-1}^{0} + i\frac{\partial\zeta}{\partial n}$$

$$= -i\left(\tau - \frac{e^{i\theta_0}}{k\alpha}\right) + i\frac{\partial\zeta}{\partial n}. \tag{18}$$

Eq. (18) expresses the fact that the vertically-integrated volume flux M is in a direction 90° clockwise (in the Northern Hemisphere) from the resultant of the surface stress τ, the bottom stress $-e^{i\theta_0}/k\alpha$, and the horizontal pressure gradient $-\partial\zeta/\partial n$. The continuity equation (1), after integrating over depth, implies that for steady motion

$$\mathrm{div} M = \frac{\partial M_x}{\partial x} + \frac{\partial M_y}{\partial y} = 0, \tag{19}$$

so we can introduce a streamfunction $\psi(x,y)$ for M_x and M_y, with

$$M_x = \frac{\partial\psi}{\partial y}, \quad M_y = -\frac{\partial\psi}{\partial x}. \tag{20}$$

We can obtain an explicit expression for $e^{i\theta_0}$ from Eq. (16) and substitute it into (18) in order to obtain

$$\frac{\partial\zeta}{\partial x} + i\frac{\partial\zeta}{\partial y} = A\left(\frac{\partial\psi}{\partial y} - i\frac{\partial\psi}{\partial x}\right) + B(\tau_x + i\tau_y), \tag{21}$$

where

$$\left.\begin{aligned} A &= \frac{iU}{U+1} \\ B &= \frac{\sqrt{\alpha}(U+1)}{\sqrt{\alpha}U + iV} \end{aligned}\right\}, \tag{22}$$

where $U = U(\alpha,\epsilon)$ and $V = V(\alpha)$ are given in (17).

We can eliminate either ψ or ζ from (21) to form a single, real, second-order elliptic equation. Here we choose to eliminate ζ, since the lateral boundary

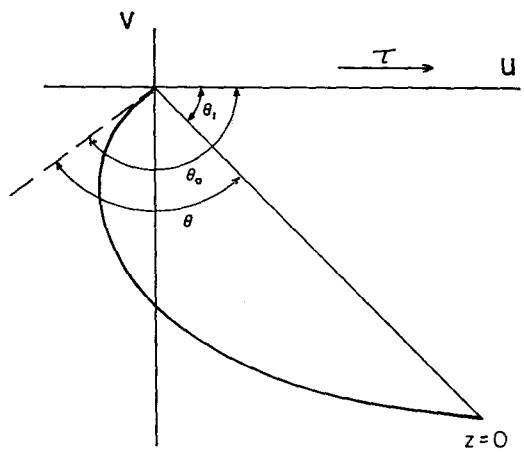

FIG. 2. Definition of the angles θ_0, θ_1 and $\theta = \theta_0 - \theta_1$ for a typical hodograph of the vertical distribution of horizontal velocity. The wind stress τ is in the positive x direction.

TABLE 2. The variation of α, θ_0, θ_1 and θ with ϵ for fixed values of τ.*

τ	ϵ	α	h/D	θ_0	θ_1	θ
1.35	0.1	0.640	0.255	− 39.50	−34.60	− 4.90
1.35	0.01	0.276	0.167	− 47.14	−38.23	− 8.91
1.35	0.001	0.164	0.129	− 45.80	−39.13	− 6.67
1.35	0.0001	0.116	0.108	− 44.13	−39.66	− 4.47
9.99	0.1	4.00	0.637	− 91.01	−51.95	− 39.06
9.99	0.01	2.71	0.524	−129.92	−54.75	− 75.17
9.99	0.001	1.69	0.414	−120.92	−58.78	− 62.14
9.99	0.0001	1.18	0.346	−113.38	−61.92	− 51.46
42.95	0.1	7.84	0.891	−132.39	−49.19	− 83.20
42.95	0.01	7.26	0.858	−197.30	−49.20	−148.10
42.95	0.001	5.09	0.718	−188.25	−50.13	−138.12
42.95	0.0001	3.92	0.630	−174.50	−51.11	−123.39
694.72	0.1	19.36	1.40	−241.70	−47.50	−194.27
694.72	0.01	21.64	1.48	−324.68	−47.35	−277.33
694.72	0.001	17.64	1.34	−336.21	−47.63	−288.58
694.72	0.0001	14.80	1.23	−320.14	−47.90	−272.24

* Angles in degrees.

condition is more easily expressed in terms of ψ. Let $A=A_R+iA_I$, $B=B_R+iB_I$, and then eliminate ζ; the result is

$$A_R\left(\frac{\partial^2\psi}{\partial x^2}+\frac{\partial^2\psi}{\partial y^2}\right)+\left(\frac{\partial A_R}{\partial x}+\frac{\partial A_I}{\partial y}\right)\frac{\partial\psi}{\partial x}+\left(\frac{\partial A_R}{\partial y}-\frac{\partial A_I}{\partial x}\right)\frac{\partial\psi}{\partial y}$$

$$=\frac{\partial}{\partial x}(B_R\tau_y+B_I\tau_x)-\frac{\partial}{\partial y}(B_R\tau_x-B_I\tau_y). \quad (23)$$

Eq. (23) is to be solved subject to the condition of no flow normal to the boundary ($\psi=0$ on the boundary). Or, changes in ψ along the boundary may be specified to represent inflows or outflows. Eq. (23) is similar in form to the corresponding equation in the case of constant vertical eddy viscosity. There is one very important difference, however; Eq. (23) is quasi-linear, rather than linear. The coefficients depend on α, which in turn depends on the solution ζ itself through the surface boundary condition (16). Since (16) is transcendental in α, the nonlinearity cannot be shown explicitly in (23). Thus, we must consider Eq. (16) along with (23) as our basic equation.

For a realistic model basin, (23) might be solved on a finite-difference grid as follows. From an initial guess at the solution, $\psi_0(x,y)$, $\zeta_0(x,y)$, the parameter $\alpha=\alpha(x,y)$ is determined at each grid point through (16). Using the values of $\alpha(x,y)$ thus determined, the coefficients A_R, A_I, B_R, B_I are determined from (22). With these coefficients specified, Eq. (23) may be treated as a linear equation in ψ and a new solution $\psi_1(x,y)$ may be generated by a standard method (e.g., successive overrelaxation). The procedure is then repeated; in general, the ith iteration, $\psi_i(x,y)$, is used to determine the coefficients in (23) in order to generate the $(i+1)$st iteration, $\psi_{i+1}(x,y)$. Because of the implicit dependence of the coefficients on the solution, it is not possible to

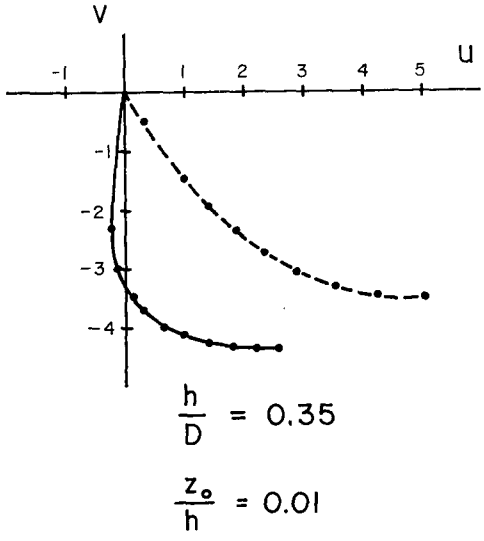

FIG. 3. Hodograph of horizontal velocity for the case $\alpha=1.21$ ($h/D=0.35$), $\epsilon=z_0/h=0.01$ (solid line), and that for the case $\nu=$constant, the same value of h/D, and the same wind stress (dashed line). The dots on each curve are at intervals of 0.1 in z.

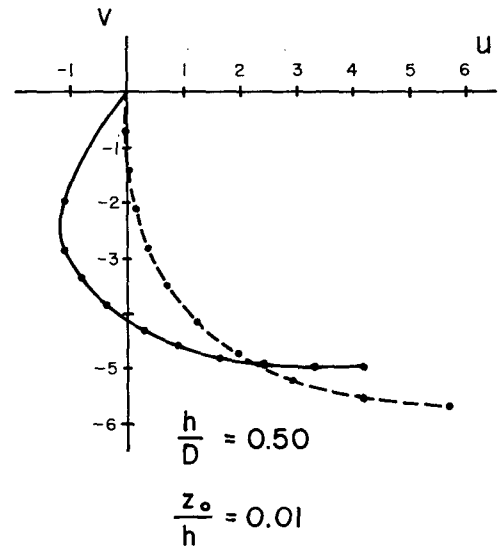

FIG. 4. As in Fig. 3., except with $\alpha=2.48$ ($h/D=0.50$).

formulate explicit conditions for convergence of this computational scheme.

3. Pure drift current

In order to illustrate the effect of the assumption of a linearly varying eddy viscosity, we consider the pure drift current in a shallow body of water with constant depth and infinite horizontal extent, in the absence of surface slopes. The results will be compared to those for a constant vertical eddy viscosity.

With zero surface slopes, the surface boundary condition (16) reduces to

$$-\frac{2}{k}i^{\frac{1}{2}}e^{i\theta_0}U(\alpha,\epsilon)=\sqrt{\alpha}\tau, \tag{24}$$

and the solution (15) reduces to

$$\phi(\eta)=\frac{\sqrt{\alpha}\tau}{i^{\frac{1}{2}}}\left\{\frac{[\tfrac{1}{2}\ln(\alpha\epsilon)+i(\pi/4)+\gamma]I_0([4i\alpha(z+1)]^{\frac{1}{2}})+K_0([4i\alpha(z+1)\tau]^{\frac{1}{2}})}{U(\alpha,\epsilon)}\right\}, \tag{25}$$

where we have eliminated θ_0 through the use of (24).

For a given surface wind stress τ and bottom roughness length ϵ, the parameters α and θ_0 are computed from (24), and the velocity distribution is then given by (25). Computationally, it is easier to fix α and ϵ, and then compute θ_0 and τ in (24). By repeating this for a range of values of α, the dependence of α on τ can be determined.

Table 1 shows values of α and τ, along with values of the angles θ_0 and θ_1 (see Fig. 2), for the case $\epsilon=z_0/h=0.01$, i.e., a roughness length equal to 1% of the depth. The surface stress has been taken to be in the positive x direction, i.e., $\tau=\tau_x$. Since the depth h is constant, $\alpha=fh^2/\nu_0$ is inversely proportional to the maximum eddy viscosity ν_0. In order to compare these results with the case of constant eddy viscosity, it is useful to introduce the concept of "friction depth." For $\nu=$ constant, the friction depth D is defined as $D=\pi(2\nu/f)^{\frac{1}{2}}$. For the variable eddy viscosity considered here, we define D in terms of the mean eddy viscosity $\nu_0/2$, and thus take $D=\pi(\nu_0/f)^{\frac{1}{2}}$. An important measure of the influence of vertical friction is then given by the

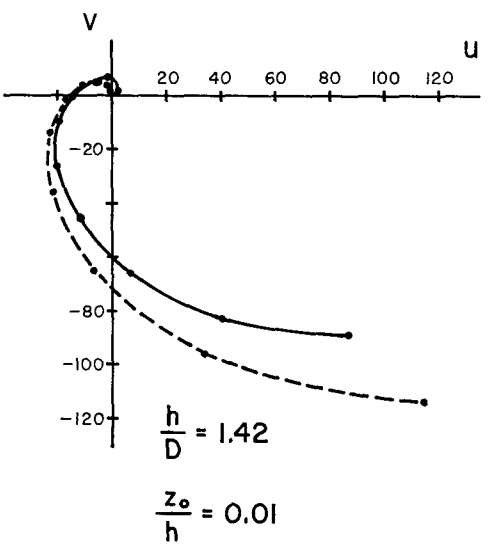

FIG. 5. As in Fig. 3., except with $\alpha=20.0$ ($h/D=1.42$).

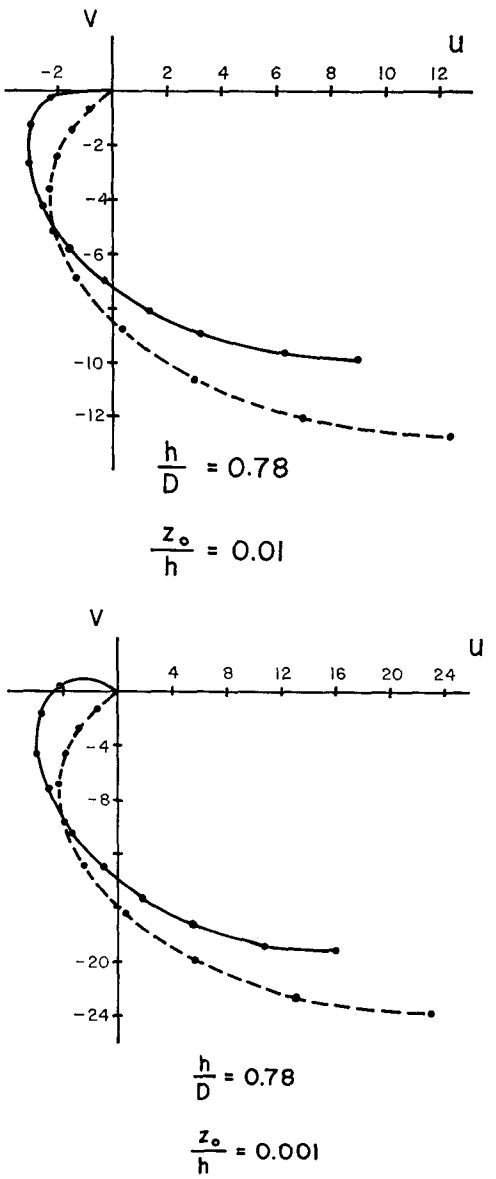

FIG. 6. As in Fig. 3., with $\alpha=6.0$ ($h/D=0.78$), for two values of $\epsilon=z_0/h$: (a) $\epsilon=0.01$, (b) $\epsilon=0.001$. Note that a change in ϵ, with α fixed, means a change in the wind stress τ and the magnitude of u and v.

ratio of total depth to friction depth, given by $h/D=\alpha^{\frac{1}{2}}/\pi$. Values of h/D are also given in Table 1.

The effect of varying the nondimensional bottom roughness length ϵ on the values of α and the angles θ_0 and θ_1, for a fixed value of τ, is shown in Table 2, for selected values of τ.

Figs. 3–5 show hodographs of the velocity distribution for different values of h/D and ϵ. Also shown in these figures, for comparison, is the velocity distribution for the case of a constant eddy viscosity equal to the mean of the variable eddy viscosity, i.e., for $\nu=\nu_0/2$ (and hence the same friction depth), and for the same surface wind stress. The cases of variable and constant ν differ considerably in shallow water ($h/D<1$, Figs. 3 and 4), but become more nearly the same in deeper water ($h/D>1$, Fig. 5). The direction of the bottom current is always displaced more from the wind direction in the case of variable ν.

Note in Table 1 that θ_1, the angular displacement of the surface current from the wind direction, increases with increasing h/D to a maximum of about 59° at $h/D=0.35$ (see Fig. 3), and then decreases slowly. The angular displacement of the bottom current, θ_0, increases with increasing h/D.

Fig. 6 shows the effect of a change in the bottom roughness. Reducing the bottom roughness length z_0 produces an effect similar to reducing the friction depth (cf. Fig. 5). In modeling a real basin, z_0 as well as h may vary with horizontal position.

Acknowledgments. I would like to thank Alan J. Witten and Stanley C. Perkins for help with the numerical computations. Prof. Alfred Clark, Jr., kindly read and commented on the manuscript. This work was supported by the National Science Foundation under Grant GA-32209.

REFERENCES

Bonham-Carter, G., and J. H. Thomas, 1973: Numerical calculation of steady wind-driven currents in Lake Ontario and the Rochester embayment. *Proc. 16th Conf. Great Lakes Research*, Intern. Assoc. Great Lakes Res., Ann Arbor, 640–652.

Caldwell, D. R., C. W. Van Atta and K. N. Helland, 1972: A laboratory study of the turbulent Ekman layer. *Geophys. Fluid Dyn.*, **3**, 125–159.

Ekman, W. V., 1905: On the influence of the earth's rotation on ocean currents. *Arkiv Mat. Astr. Fys.*, **2**, No. 11, 1–53.

Ellison, T. H., 1956: Atmospheric turbulence. *Surveys in Mechanics*, G. K. Batchelor and R. M. Davies, Eds., Cambridge University Press, 400–430.

Fjelstad, J. E., 1929: Ein Beitrag zur Theorie der winderzeugten Meeresströmungen. *Beitr. Geophys.*, **23**, 237–247.

Gedney, R. T., and W. Lick, 1972: Wind-driven currents in Lake Erie. *J. Geophys. Res.*, **77**, 2714–2723.

——, —— and F. B. Molls, 1972: Effect of eddy diffusivity on wind-driven currents in a two-layer stratified lake. NASA TN D-6841.

Welander, P., 1957: Wind action on a shallow sea: Some generalizations of Ekman's theory. *Tellus*, **9**, 45–52.